OPEN

CASE REPORT
Breast

Breast Reconstruction following Breast-conserving Surgery with a Subcutaneous Tissue Expander and Latissimus Dorsi Flap

KoichiTomita, MD, PhD
Kenji Yano, MD, PhD
Yuta Sugio, MD
Takayoshi Ishihara, MD
Akimitsu Nishibayashi, MD
Ken Matsuda, MD, PhD
Ko Hosokawa, MD, PhD

Summary: Corrective surgery following breast-conserving surgery is generally challenging due to severe fibrosis induced by postoperative radiotherapy. Although use of the latissimus dorsi myocutaneous flap offers a safe and reliable option, exposure of the skin paddle to the skin surface is often inevitable to achieve correction of nipple-areola complex malposition, leaving conspicuous, patchwork-like scars on the breast. In this report, we describe a 2-stage procedure using a subcutaneous tissue expander and the latissimus dorsi myocutaneous flap for the correction of both nipple-areola complex malposition and breast volume without skin paddle exposure. Although careful observation is necessary during skin expansion, this technique could offer an alternative option for patients undergoing corrective surgery following breast-conserving surgery. *(Plast Reconstr Surg Glob Open 2014;2:e231; doi: 10.1097/GOX.0000000000000200; Published online 10 October 2014.)*

Breast-conserving surgery (BCS) has been widely accepted given the high survival rate comparable to that of radical mastectomy and as it allows for preservation of a large proportion of the breast.[1] Yet, roughly 30% of patients are reportedly unsatisfied with the cosmetic outcomes of BCS.[2] The correction of cosmetic sequelae, however, is usually challenging for reconstructive surgeons due to severe fibrosis induced by postoperative radiotherapy.[3]

Correction of breast deformity following BCS normally uses the latissimus dorsi myocutaneous (LDM) flap for its reliable vascularity, low complication rate, and technical ease.[4–6] Although aesthetic improvements can often be achieved, exposure of the skin paddle to the skin surface during the correction of nipple-areola complex (NAC) malposition is inevitable in most cases.[7] Because the texture of the back skin differs considerably from that of the breast skin, patchwork-like breast scars are often conspicuous. To address this issue, contractures of skin and soft tissue should be released before LDM flap reconstruction.

Here, we report a case in which a subcutaneous tissue expander (TE) was used before LDM flap transfer, leading to a successful correction of NAC malposition and breast volume without skin paddle exposure.

From the Department of Plastic and Reconstructive Surgery, Graduate School of Medicine, Osaka University, Osaka, Japan.
Received for publication August 9, 2014; accepted August 25, 2014.

DOI: 10.1097/GOX.0000000000000200

CASE REPORT

A 52-year-old woman underwent BCS due to breast cancer in the right upper quadrants at another hospital. Eleven years later, she visited our clinic

Disclosure: *The authors have no financial interest to declare in relation to the content of this article. The Article Processing Charge was paid for by a grant from the Japanese Ministry of Education, Science, Sports and Culture (25462789).*

to correct the cosmetic sequelae of BCS. The initial examination revealed severe right breast deformity and NAC malposition (Fig. 1). The volume difference between the right and left breasts was estimated to be about 220 cm^3 based on 3-dimensional computer analysis (Breast-Rugle, Medic Engineering, Kyoto, Japan) (Fig. 2). To correct NAC malposition and breast volume without exposing the skin paddle, we performed a 2-stage procedure using a subcutaneous TE and the LDM flap.

First, a rectangular TE (Integra, Model No. 3610-44-2, PMT Corporation, Chanhassen, Minn.) was inserted into a subcutaneous pocket created in the upper quadrants to correct the cranially malpositioned NAC. Although a part of the breast skin became very thin during expansion, the TE could be filled up to 325 cm^3 (Fig. 3). Five months later, reconstruction with the LDM flap was performed. The flap weighing about 280 g was elevated in the left lateral decubitus position, and the TE was replaced with the LDM flap in the sitting position. Before placing the LDM flap in the pocket, extensive capsulotomy was performed to release residual contractures of the skin and soft tissue.

The postoperative course was uneventful, and the patient was satisfied with the aesthetic outcome. Postoperative photographs show that NAC malposition is well corrected, and the breast scar is inconspicuous (Fig. 4). Postoperative 3-dimensional analysis also revealed that the right and left breasts are similar in both overall and regional breast volumes.

DISCUSSION

Correction of breast deformity following BCS with a local flap, fat grafting, or an implant is associated with a high rate of postoperative complications due to initial radiotherapy.[8–10] The LDM flap has high vascularity and is associated with fewer risk factors, and therefore, it will likely afford improved aesthetic

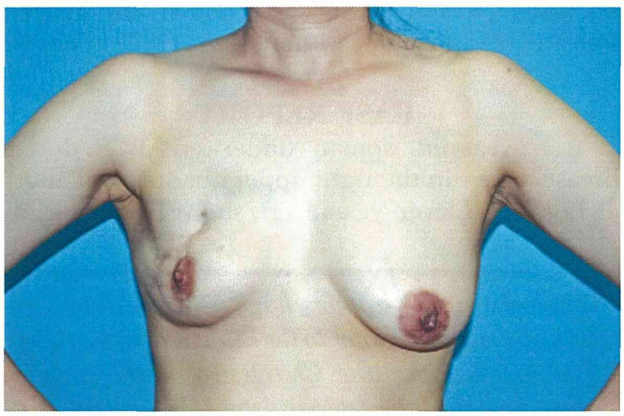

Fig. 1. Preoperative frontal view of the patient. Severe malpositioning of the nipple-areola complex is noted.

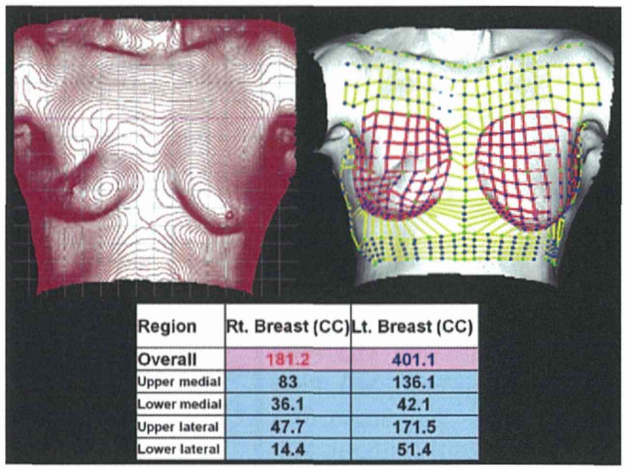

Fig. 2. Preoperative 3-dimensional computer analysis revealed that the estimated volume difference between the right and left breasts was about 220 cm^3.

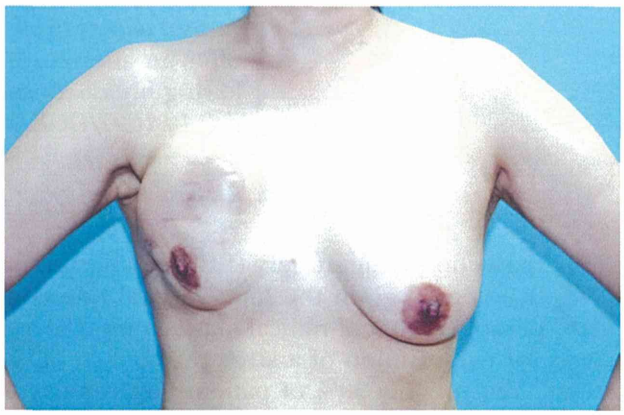

Fig. 3. In the first stage, a rectangular tissue expander was placed in a subcutaneous pocket created in the upper quadrants. Although a part of the skin became very thin, the tissue expander could be filled up to 325 cm^3.

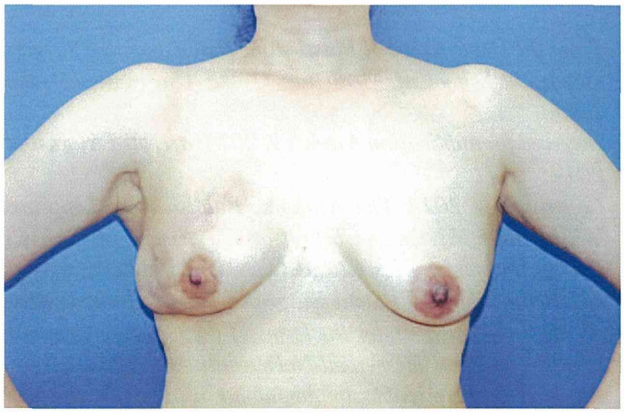

Fig. 4. Postoperative (5 months) frontal view of the patient is shown. Note that malpositioning of the nipple-areola complex is well corrected.

outcomes.[7] However, exposure of the skin paddle to the skin surface is inevitable when correcting NAC malposition, leaving conspicuous, patchwork-like scars on the reconstructed breast.

In the present case, we used a subcutaneous TE before LDM flap transfer to release skin contracture. Correction of both breast volume and NAC malposition was achieved without skin paddle exposure. Compared with subpectoral TE placement, subcutaneous TE placement not only allows for better control of breast shape[11] but also provides increased TE stability, preventing TE movement during expansion. Of course, careful observation of the skin condition is necessary during expansion, but in our case, sufficient skin expansion was achieved without any major complications.

We used a smooth, rectangular TE in the present case, but there remains room for discussion regarding the type of TE that is suitable for each case. For instance, a textured TE might cause less capsular contracture and less resistance to expansion,[12] whereas a recently developed tabbed TE might provide more stability even in the case of subpectoral TE placement.[13] Further studies are needed to address these issues.

CONCLUSIONS

Although correction of breast deformity after BCS with severe malpositioning of the NAC is challenging, our 2-stage procedure using a subcutaneous TE and the LDM flap could achieve correction of both NAC malposition and breast volume without leaving conspicuous, patchwork-like scars on the reconstructed breast. Although careful observation is required during skin expansion, and further studies are warranted regarding the suitable type of TE, this method offers a good alternative for patients undergoing corrective surgery after BCS.

Koichi Tomita, MD, PhD
Department of Plastic and Reconstructive Surgery
Graduate School of Medicine, Osaka University
2-2 Yamadaoka, Suita
Osaka 5650871, Japan
E-mail: ktomita9@hotmail.co.jp

REFERENCES

1. Fisher B, Anderson S, Bryant J, et al. Twenty-year follow-up of a randomized trial comparing total mastectomy, lumpectomy, and lumpectomy plus irradiation for the treatment of invasive breast cancer. *N Engl J Med.* 2002;347:1233–1241.
2. Urban C, Lima R, Schunemann E, et al. Oncoplastic principles in breast conserving surgery. *Breast* 2011;20(Suppl 3):S92–S95.
3. Clough KB, Cuminet J, Fitoussi A, et al. Cosmetic sequelae after conservative treatment for breast cancer: classification and results of surgical correction. *Ann Plast Surg.* 1998;41:471–481.
4. Tomita K, Yano K, Masuoka T, et al. Postoperative seroma formation in breast reconstruction with latissimus dorsi flaps: a retrospective study of 174 consecutive cases. *Ann Plast Surg.* 2007;59:149–151.
5. Tomita K, Yano K, Matsuda K, et al. Esthetic outcome of immediate reconstruction with latissimus dorsi myocutaneous flap after breast-conservative surgery and skin-sparing mastectomy. *Ann Plast Surg.* 2008;61:19–23.
6. Tomita K, Yano K, Hosokawa K. Recovery of sensation in immediate breast reconstruction with latissimus dorsi myocutaneous flaps after breast-conservative surgery and skin-sparing mastectomy. *Ann Plast Surg.* 2011;66: 334–338.
7. Tomita K, Yano K, Nishibayashi A, et al. The role of latissimus dorsi myocutaneous flaps in secondary breast reconstruction after breast-conserving surgery. *Eplasty* 2013;13:e28.
8. Kronowitz SJ, Robb GL. Radiation therapy and breast reconstruction: a critical review of the literature. *Plast Reconstr Surg.* 2009;124:395–408.
9. Hirsch EM, Seth AK, Dumanian GA, et al. Outcomes of tissue expander/implant breast reconstruction in the setting of prereconstruction radiation. *Plast Reconstr Surg.* 2012;129:354–361.
10. Uda H, Sugawara Y, Sarukawa S, et al. Brava and autologous fat grafting for breast reconstruction after cancer surgery. *Plast Reconstr Surg.* 2014;133:203–213.
11. Tadiparthi S, Alrawi M, Collis N. Two-stage delayed breast reconstruction with an expander and free abdominal tissue transfer: outcomes of 65 consecutive cases by a single surgeon. *J Plast Reconstr Aesthet Surg.* 2011;64:1608–1612.
12. Barone FE, Perry L, Keller T, et al. The biomechanical and histopathologic effects of surface texturing with silicone and polyurethane in tissue implantation and expansion. *Plast Reconstr Surg.* 1992;90:77–86.
13. Spear SL, Economides JM, Shuck J, et al. Analyzing implant movement with tabbed and nontabbed expanders through the process of two-stage breast reconstruction. *Plast Reconstr Surg.* 2014;133:256e–260e.

Biochemical and Biophysical Research Communications 454 (2014) 12–18

Contents lists available at ScienceDirect

Biochemical and Biophysical Research Communications

journal homepage: www.elsevier.com/locate/ybbrc

Cyp26b1 within the growth plate regulates bone growth in juvenile mice

Yoshiki Minegishi [a,b,c], Yasuo Sakai [c,d], Yasuhito Yahara [a], Haruhiko Akiyama [e], Hideki Yoshikawa [f], Ko Hosokawa [c], Noriyuki Tsumaki [a,g,*]

[a] Department of Cell Growth and Differentiation, Center for iPS Cell Research and Application, Kyoto University, 53 Kawahara-cho, Shogoin, Sakyo-ku, Kyoto 606-8507, Japan
[b] Department of Plastic and Reconstructive Surgery, University of Fukui Hospital, 23-3 Matsuokashimoaizuki, Eiheiji-cho, Yoshida-gun, Fukui 910-1193, Japan
[c] Department of Plastic Surgery, Osaka University Graduate School of Medicine, 2-2 Yamadaoka, Suita, Osaka 565-0871, Japan
[d] Department of Plastic Surgery, Bellland General Hospital, 500-3 Higashiyama Naka-ku, Sakai, Osaka 599-8247, Japan
[e] Department of Orthopaedic Surgery, Gifu University Graduate School of Medicine, 1-1 Yanagito, Gifu 501-1194, Japan
[f] Department of Orthopaedic Surgery, Osaka University Graduate School of Medicine, 2-2 Yamadaoka, Suita, Osaka 565-0871, Japan
[g] Japan Science and Technology Agency, CREST, Tokyo 102-0075, Japan

ARTICLE INFO

Article history:
Received 20 September 2014
Available online 8 October 2014

Keywords:
Retinoic acid
Growth plate
Cyp26b1
Chondrocytes

ABSTRACT

Retinoic acid (RA) is an active metabolite of vitamin A and plays important roles in embryonic development. CYP26 enzymes degrade RA and have specific expression patterns that produce a RA gradient, which regulates the patterning of various structures in the embryo. However, it has not been addressed whether a RA gradient also exists and functions in organs after birth. We found localized RA activities in the diaphyseal portion of the growth plate cartilage were associated with the specific expression of *Cyp26b1* in the epiphyseal portion in juvenile mice. To disturb the distribution of RA, we generated mice lacking *Cyp26b1* specifically in chondrocytes (*Cyp26b1*$^{\Delta chon}$ cKO). These mice showed reduced skeletal growth in the juvenile stage. Additionally, their growth plate cartilage showed decreased proliferation rates of proliferative chondrocytes, which was associated with a reduced height in the zone of proliferative chondrocytes, and closed focally by four weeks of age, while wild-type mouse growth plates never closed. Feeding the *Cyp26b1* cKO mice a vitamin A-deficient diet partially reversed these abnormalities of the growth plate cartilage. These results collectively suggest that Cyp26b1 in the growth plate regulates the proliferation rates of chondrocytes and is responsible for the normal function of the growth plate and growing bones in juvenile mice, probably by limiting the RA distribution in the growth plate proliferating zone.

1. Introduction

Retinoic acid (RA) is an active metabolite of vitamin A and plays important roles in embryonic development. The concentration of RA is controlled by the balance between its synthesis by retinaldehyde dehydrogenase (RALDH) and its degradation by CYP26 enzymes. CYP26s are a group of P450 enzymes that metabolize RA to inactive forms [1–3]. Both RALDH and Cyp26 have specific expression patterns and produce a RA gradient [4]. This RA gradient regulates the patterning of the anterior–posterior axis of various structures, including the hindbrain and paraxial mesoderm [5]. The RA gradient also regulates the proximodistal patterning and outgrowth of the developing limbs. *Cyp26b1* is expressed in the distal region of developing limb buds, and mice that lack *Cyp26b1* show severe limb malformation due to the spreading of the RA signal toward the distal end of the developing limb, causing abnormal patterning of limb skeletal elements [6]. However, whether this RA gradient also regulates the growth and maintenance of organs after birth has not been addressed.

The growth plate cartilage is where bone growth occurs in juveniles. Growth plate cartilage is located in the metaphysis at each end of long bones. Chondrocytes residing at the epiphyseal side in the growth plate cartilage proliferate and subsequently undergo hypertrophy just after stopping proliferation. As a result, chondrocytes change from proliferating chondrocytes on the

Abbreviations: RA, retinoic acid; *RARE*, RA-responsive elements; *Cyp26b1*$^{\Delta chon}$ cKO, *11Enh-Cre Cyp26b1*$^{flox/flox}$ conditional knockout.

* Corresponding author at: Department of Cell Growth and Differentiation, Center for iPS Cell Research and Application, Kyoto University, 53 Kawahara-cho, Shogoin, Sakyo-ku, Kyoto 606-8507, Japan. Fax: +81 75 366 7047.
E-mail address: ntsumaki@cira.kyoto-u.ac.jp (N. Tsumaki).

http://dx.doi.org/10.1016/j.bbrc.2014.10.001
0006-291X/

epiphyseal side to hypertrophic chondrocytes on the diaphyseal side of growth plate cartilage. The hypertrophic chondrocytes residing at the diaphyseal end of the growth plate cartilage subsequently die, and the hypertrophic cartilage is degraded and gradually replaced by bone. Through this mechanism, the bone becomes elongated. Thus, strict regulation of chondrocyte proliferation and hypertrophic differentiation is necessary for the normal growth of bones.

In juveniles, focal closures of the growth plate in the distal tibia [7], the proximal tibia [8], the distal tibia, elbow, proximal femur and distal femur [9] are caused by the treatment of acne with retinoids [7] or the treatment of hyperkeratinosis with cis-retinoic acid [8,9]. In guinea pigs, the application of RA caused closure of the growth plates in the proximal tibia [10]. These clinical and preclinical manifestations indicate that vitamin A and its metabolites play important roles in the bone growth of juveniles. The RA signal has been shown to regulate bone growth after birth. The deletion of RA receptors (RAR) in chondrocytes disturbs skeletal growth due to abnormal chondrocyte differentiation and disturbed matrix synthesis within the growth plates in mice [11]. Additionally, a localized distribution of RA was detected in the growth plate cartilage of the ribs of three-week-old rabbits [12]. However, it remains to be determined how RA regulates the bone growth of juveniles. In this study, we found that the expression of Cyp26b1 specifically in the proliferative chondrocyte zone was associated with localized RA activities in the zone of hypertrophic chondrocytes in the growth plate cartilage of juvenile mice. To disturb the distribution of RA, we inactivated Cyp26b1 in the growth plate using Cyp26b1 conditional knock-out mice. The resulting mouse phenotype suggests that Cyp26b1 within the growth plate regulates the proliferation rates of chondrocytes and bone growth in juveniles.

2. Materials and methods

2.1. Animals and PCR genotyping procedures

RARE-LacZ mice were a gift from Dr. Janet Rossant [13]. To generate *Cyp26b1* conditional knockout mice, *11Enh-Cre* transgenic mice [14,15] and *Cyp26b1*$^{flox/flox}$ mice [16] were prepared and mated to generate *11Enh-Cre; Cyp26b1*$^{flox/+}$ mice. Then, the *11Enh-Cre; Cyp26b1*$^{flox/+}$ and *Cyp26b1*$^{flox/flox}$ mice were intercrossed, and the *11Enh-Cre; Cyp26b1*$^{flox/flox}$ mice were considered conditional knockout (*Cyp26b1*$^{\Delta chon}$ cKO) mice. The *11Enh-Cre; Cyp26b1*$^{flox/+}$ mice were used as controls.

For genotyping, genomic DNA was isolated from the tail tips or embryonic skin and subjected to PCR analysis, according to a previously described method for the *Cre* transgene [14] and *Cyp26b1* allele [16].

2.2. Frozen sectioning and laser capture microdissection (LMD)

Mouse hindlimbs were harvested without fixation and were immediately embedded in SCEM compound (SECTION-LAB, Hiroshima, Japan). Frozen sections were prepared at 6-μm thickness with a Cryofilm type 2c(9) (SECTION-LAB) using a CM3050S cryomicrotome (Leica), according to the method described by Kawamoto [17]. The sections were briefly fixed with 100% ethanol. Semiserial sections were then stained with hematoxylin and eosin.

For LMD, frozen sections were prepared with LMD film (SECTION-LAB) using a cryomicrotome. The sections were freeze-dried in the cryostat chamber at −25 °C for one hour and briefly fixed with 100% ethanol. The proliferative zone and hypertrophic zone in the growth plate were individually captured and microdissected from cryosections using a Leica LMD7000 device (Leica) and put onto the dip of the lid of 0.5 ml tubes with cold TRIzol (Life Technologies, Tokyo, Japan).

2.3. Real-time RT-PCR

RNA was extracted from the collected samples using RNeasy Mini Kits (Qiagen, Tokyo, Japan). The total RNA was digested with DNase to eliminate any contaminating genomic DNA. For real-time quantitative RT-PCR analyses, 1 μg of total RNA was reverse-transcribed into first-strand cDNA using ReverTra Ace (Toyobo, Osaka, Japan) and random primers. The PCR amplification was performed in a reaction volume of 20 μl containing 2 μl of cDNA, 10 μl of SYBR FAST qPCR Master Mix (Kapa Biosystems, Tokyo, Japan) and 7900HT (Applied Biosystems). The RNA expression levels were normalized to the level of *Gapdh* expression. The primers used are listed in Table 1.

2.4. Staining of the skeleton

Mouse limbs were dissected, fixed in 100% ethanol overnight and then stained with Alcian blue, followed by Alizarin red S solution, according to standard protocols [18].

2.5. Histological analysis

Mouse limbs were dissected, fixed in 4% paraformaldehyde, processed and embedded in paraffin. For the immunohistochemical analysis, sections were incubated with an anti-CYP26B1 antibody (Scrum Inc., Tokyo, Japan) and an anti-type X collagen antibody (COSMO BIO CO., Ltd., Tokyo, Japan). Immune complexes were detected using secondary antibodies conjugated to Alexa Fluor 555 and Alexa Fluor 546, respectively.

2.6. BrdU staining

Mice were intraperitoneally injected with BrdU labeling reagent (10 μl/g body weight) (Zymed Laboratories Inc., South San Francisco, CA) two hours before being sacrificed. The mice were then dissected and sectioned. The incorporated BrdU was detected using a BrdU staining kit (Zymed Laboratories, Inc., South San Francisco, CA) to distinguish actively proliferating cells. The mean number of BrdU-positive cells/total cells ± standard deviation (S.D.) was calculated.

2.7. Microscope

Images were acquired on an inverted microscope (Eclipse Ti; Nikon) equipped with cameras (DS-Fi1; Nikon and C4742-80-12AG; Hamamatsu photonics) and the NIS Elements software program (Nikon).

Table 1
Primer sequences used in this study.

Primer	Sequence (5′–3′)
Col2a1 S	TTGAGACAGCACGACGTGGAG
Col2a1 AS	AGCCAGGTTGCCATCGCCATA
Col10a1 S	GGTGTGAATGGGCGGAAAG
Col10a1 AS	GCTTCCCAATACCTTCTCGTC
MMP13 S	TGTTTGCAGAGCACTACTTGAA
MMP13 AS	CAGTCACCTCTAAGCCAAAGAAA
Runx2 S	CCGCACGACAACCGCACCAT
Runx2 AS	CGCTCCGGCCCACAAATCTC
Beta galactosidase S	CTCAAACTGGCAGATGCACGGT
Beta galactosidase AS	CGTTGCACCACAGATGAAACGC
Cyp26b1 S	GCAAGATCCTACTGGGCGAAC
Cp26b1 AS	TTGGGCAGGTAGCTCTCAAGT
Gapdh S	AAGCCCATCACCATCTTCCAGGAG
Gapdh AS	ATGAGCCCTTCCACAATGCCAAAG

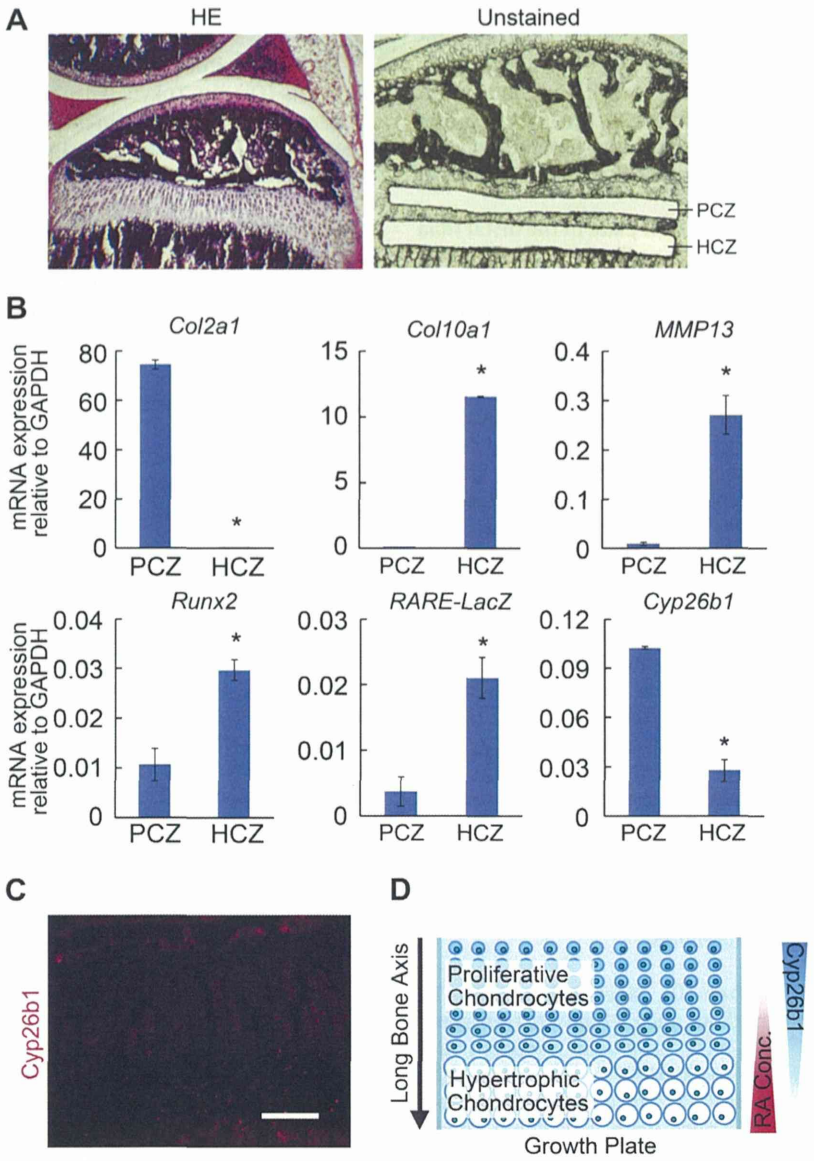

Fig. 1. Regulated RA distribution along the long axis of long bones within the growth plate cartilage. (A) We microdissected the growth plate cartilage of the proximal tibia to obtain chondrocytes from the proliferative zone (PCZ) and hypertrophic zone (HCZ) from *RARE-LacZ* mice at 2.5 weeks after birth. *Left*, a semiserial section was stained with hematoxylin and eosin. *Right*, a residual section after microdissection. (B) RNAs were extracted from cells in the proliferative chondrocyte zone (PCZ) and cells in the hypertrophic chondrocyte zone (HCZ), which were respectively obtained by microdissection, and were subjected to a real-time RT-PCR expression analysis for the genes indicated at the top of each graph. $^{*}P < 0.01$ ($n = 5$). (C) Histological sections of growth plate cartilage from the proximal tibias from three-week-old mice were immunostained with an anti-CYP26B1 antibody (Red). Bar: 100 μm. (D) A schematic representation of the RA concentration and *Cyp26b1* expression within the growth plate cartilage. Regulated RA activities were found along the long axis of the long bone within the growth plate cartilage and attributed to the localized expression of CYP26B1 in the proliferative chondrocyte zone.

2.8. Statistical analyses

Data are shown as the means and S.D. Student's *t*-test was used to compare data. *P* values <0.05 were considered statistically significant.

3. Results

3.1. Localized expression of Cyp26b1 and regulation of RA activities along the direction of bone elongation within the growth plate cartilage

To test our hypothesis that a RA gradient exists within the growth plate cartilage, we employed *RARE-lacZ* transgenic mice, in which *lacZ* is expressed under the control of RA-responsive elements (*RARE*) [13]. Because trabecular bone shows high background galactosidase activities, it is difficult to detect transgene-specific lacZ activities in bone, especially after birth. Therefore, we microdissected the growth plate cartilage, obtained cells from the proliferative chondrocyte and hypertrophic zones (Fig. 1A), and subjected them to an analysis of the expression of the *lacZ* transgene mRNA by real-time RT-PCR. The expression analysis of proliferative and hypertrophic chondrocyte markers confirmed that cells were isolated appropriately by microdissection (Fig. 1B). *LacZ* was much more highly expressed in the hypertrophic chondrocytes than in the proliferative chondrocytes (Fig. 1B). Interestingly, we detected a much higher level of *Cyp26b1* mRNA expression in the proliferative chondrocytes than in the

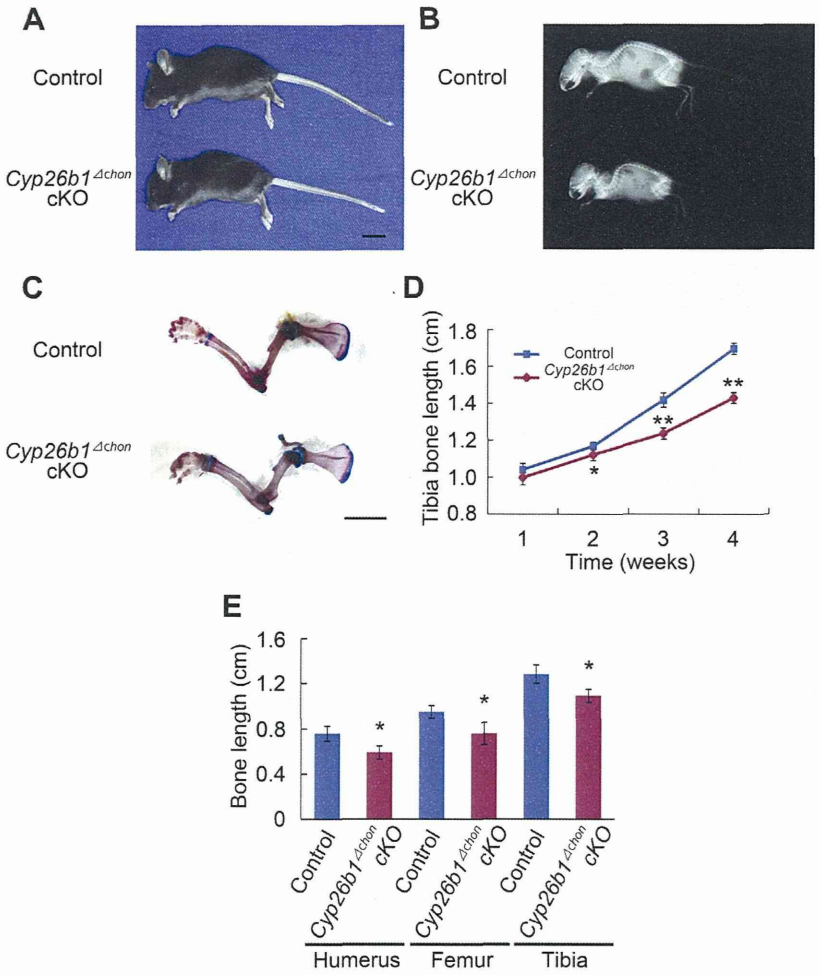

Fig. 2. The skeletal phenotype of *11Enh-Cre; Cyp26b1*$^{flox/flox}$ (*Cyp26b1*$^{\Delta chon}$) cKO mice and *11Enh-Cre; Cyp26b1*$^{flox/+}$ control mice. (A) The gross appearances of mice three weeks after birth. *Cyp26b1*$^{\Delta chon}$ cKO mice exhibited dwarfism with a short snout. Bar: 1 cm. (B) X-ray images of mice three weeks after birth. (C) The skeletons of the forelimbs of mice three weeks after birth. Alcian blue/Alizarin red staining. Bar: 5 mm. (D) The lengths of the tibiae at one, two, three and four weeks after birth. $^{/}P < 0.05$; $^{//}P < 0.01$ ($n = 5$). (E) Lengths of the humeri, femurs and tibiae three weeks after birth. $^{/}P < 0.01$ ($n = 5$).

hypertrophic chondrocytes (Fig. 1B). Accordingly, immunohistochemical analysis showed that CYP26B1 was expressed more abundantly in proliferative chondrocytes than in hypertrophic chondrocytes (Fig. 1C). These results suggest that regulated RA distribution along the direction of the bone elongation exists within the growth plate cartilage and is generated by the exclusive localization of CYP26B1 in the proliferative chondrocyte zone (Fig. 1D).

3.2. Cyp26b1 deletion in chondrocytes disturbs the bone growth in juveniles

To disturb the distribution of RA, we deleted *Cyp26b1* in the proliferative chondrocytes of the growth plate cartilage by generating *11Enh-Cre; Cyp26b1*$^{flox/flox}$ conditional knockout (*Cyp26b1*$^{\Delta chon}$ cKO) mice. The *11Enh-Cre* transgene directed Cre expression in the proliferative chondrocytes after the completion of skeletal patterning under the control of the promoter/enhancer sequence of the type XI collagen α2 chain gene (*Col11a2*) [14,15]. *Cyp26b1*$^{\Delta chon}$ cKO mice showed normal skeletal patterning, skeletal development and bone length until one week after birth. However, at three weeks after birth, they started to show a chondrodysplasia phenotype that included dwarfism and a short snout (Fig. 2A and B). A precise examination of the lengths of skeletal elements revealed a gradual decrease in the lengths of bones compared to control mice beginning from two weeks after birth (Fig. 2C–E), and all long bones in the *Cyp26b1*$^{\Delta chon}$ cKO mice were shorter than those in the controls at three weeks after birth.

To analyze the mechanism responsible for the shorter bones in the *Cyp26b1*$^{\Delta chon}$ cKO mice, we performed a histological analysis of their growth plates. We noticed a slight decrease in the height of the proliferative chondrocyte zone at two weeks after birth (Fig. 3A, top row). The height of the proliferative chondrocyte zone was significantly decreased at three weeks after birth, especially at the central portion (Fig. 3A, middle row, and Fig. 3B). Immunohistochemistry using an anti-type X collagen antibody revealed that the location of the hypertrophic cartilage zone that produced type X collagen was shifted toward the epiphysis in Cyp26b1 cKO mice, clarifying the decreased height of the zone of proliferative chondrocytes (Fig. 3C) to the central portion.

The growth plate was closed at the central portion at four weeks after birth (Fig. 3A, bottom row), and growth plate closure was recognized in all bones examined, including the tibia, humerus and femur (Fig. 3A and D). BrdU labeling analysis revealed significantly decreased proliferation rates of the proliferative chondrocytes when the mice were one and three weeks old (Fig. 4A–C). These results suggest that the decreased proliferation rates of the

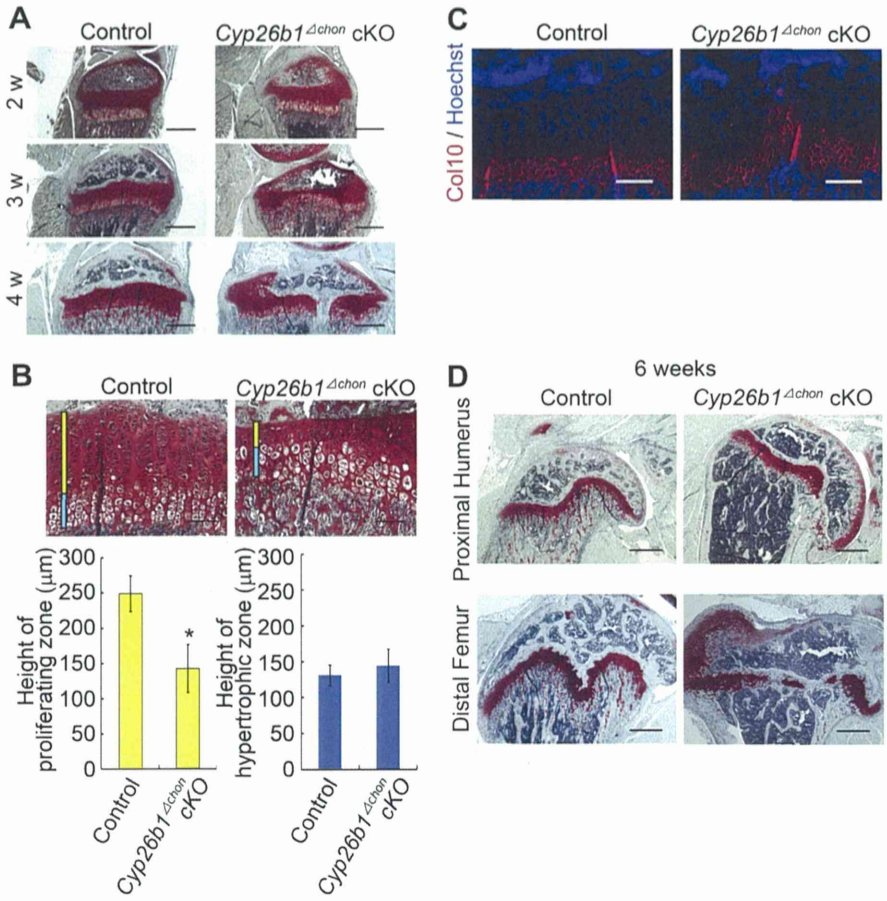

Fig. 3. Histological analysis of the growth plate cartilage of *Cyp26b1*$^{\Delta chon}$ cKO mice. (A) Sagittal sections of the proximal tibia at two, three and four weeks after birth. Safranin O-fast green-iron hematoxylin staining. Bar: 500 μm. (B) *Top*, Magnified image of the central part of the growth plate cartilage in the proximal tibia three weeks after birth. Safranin O-fast green-iron hematoxylin staining. Yellow bars indicate the height of the proliferative chondrocyte zone. Blue bars denote the height of the hypertrophic chondrocyte zone. Bars: 100 μm. Bottom, the mean ± S.D. of the height of the proliferative chondrocyte zone (left) and the hypertrophic chondrocyte zone (right). $^{*}P < 0.01$ ($n = 5$). (C) Sagittal sections of the proximal tibia at three weeks after birth were immunostained with an anti-type X collagen antibody. Bars: 100 μm. (D) Histology of the growth plate cartilage in the proximal humerus and distal femur in *Cyp26b1*$^{\Delta chon}$ cKO mice six weeks after birth. Safranin O-fast green-iron hematoxylin. Bars: 500 μm.

proliferative chondrocytes can explain the decreased heights of the proliferative chondrocyte zone, the subsequent closure of the growth plates and the suppression of bone growth.

3.3. Reversion of the growth plate abnormalities by feeding Cyp26b1$^{\Delta chon}$ *cKO mice a vitamin A-deficient diet*

The immunohistochemical analysis confirmed that CYP26B1 was absent in the proliferative chondrocytes of *Cyp26b1*$^{\Delta chon}$ cKO mice (Fig. 4D), and that this absence could cause a disturbance in the RA distribution within the growth plate.

To confirm that the elevated concentration of RA in the proliferative chondrocytes of *Cyp26b1*$^{\Delta chon}$ cKO mice was responsible for the decreased proliferation rates, we fed the mice a vitamin A-deficient diet which systemically decreased RA concentrations [19]. Following this diet, *Cyp26b1*$^{\Delta chon}$ cKO mice showed a partial reversion in the decreased proliferation rates of the proliferative chondrocytes (Fig. 4E) and corresponding partial reversion in the decreased height of the proliferative chondrocyte zone (Fig. 4F). These results collectively suggest that the distribution of RA, which is generated by the proliferative chondrocyte-specific expression of *Cyp26b1*, regulates the proliferation rates of chondrocytes and subsequently controls the growth rates and closure of growth plates to determine the length of bones in juveniles.

4. Discussion

It is well known that the RA gradient regulates the patterning of spatial structures in mammals during development. Cyp26b1 is a critical regulator of the distribution of RA, and Cyp26b1 KO and cKO studies have demonstrated that Cyp26b1 deletion alters the RA distribution in various tissues [5,16,20,21]. The present study provides evidence that Cyp26b1 within the growth plate cartilage is important for normal chondrocyte proliferation/differentiation and bone growth in juvenile mice, probably through its regulation of the RA distribution in the growth plate.

We detected localized RA activities within the growth plate cartilage in juvenile mice, as indicated by the increased *RARE-lacZ* expression toward hypertrophic chondrocytes (Fig. 1B). The existence of a possible RA gradient within the growth plate is supported by a previous report demonstrating that the RA content measured by MS quantification was lower in the resting and proliferative chondrocyte zone than that in the hypertrophic chondrocyte zone in the growth plate cartilage of the ribs of three-week old rabbits [12]. It was reported that *RARE-lacZ* expression is not

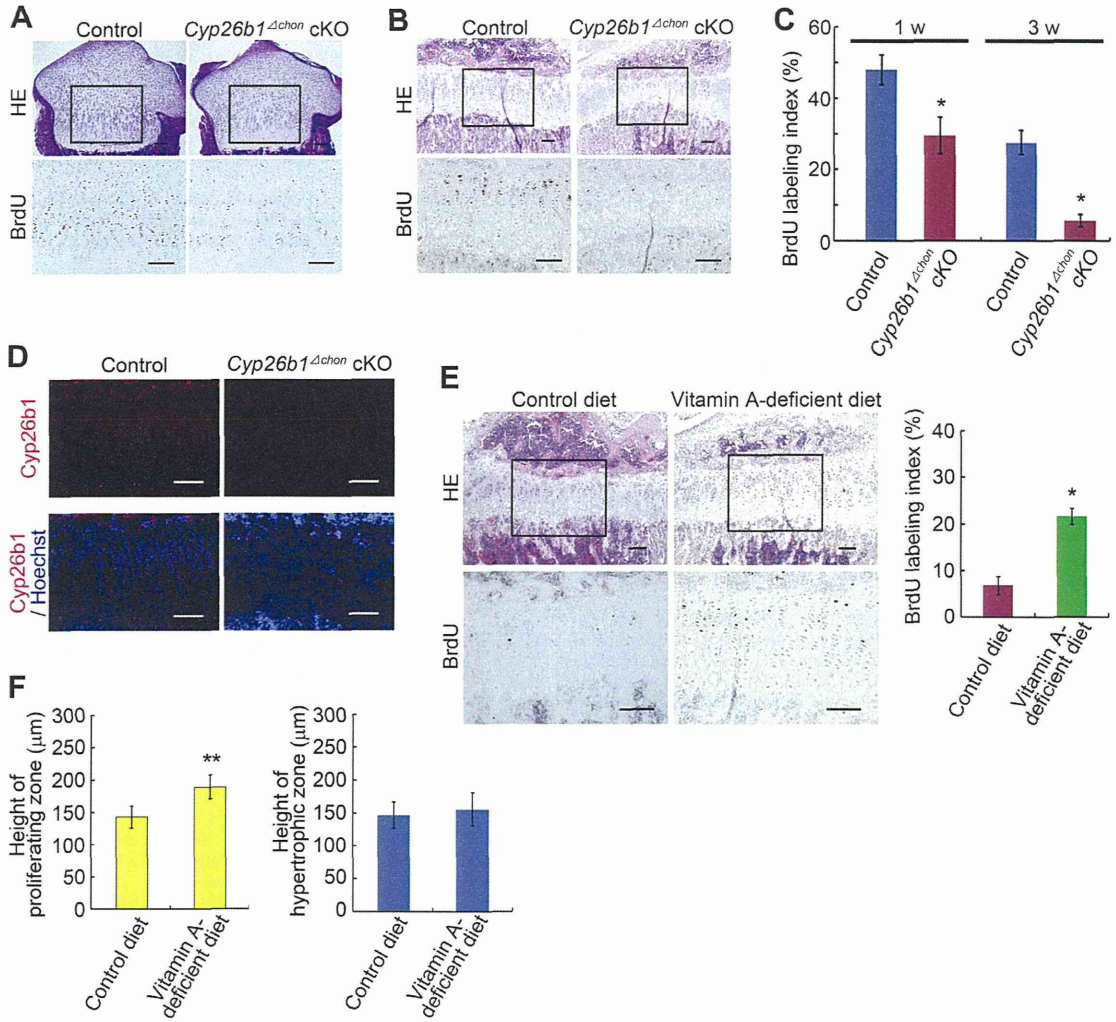

Fig. 4. Proliferation rates and Cyp26b1 expression of chondrocytes in the growth plate cartilage, and the effects of a vitamin A-deficient diet on the growth plate cartilage in the proximal tibias of *Cyp26b1*$^{\Delta chon}$ cKO mice. (A, B, C) BrdU was injected intraperitoneally into the mice two hours before sacrifice. One-week old mice (A) and three-week old mice (B). Top, hematoxylin–eosin staining. Bottom, semiserial sections were immunostained with an anti-BrdU antibody. Regions corresponding to the boxed regions in the top are magnified and shown. Bars: 100 μm. (C) Ratios (%) of the number of BrdU-positive cells to the numbers of total cells in the proliferative chondrocyte zone. $^{/}P < 0.01$ ($n = 5$). (D) Histological sections of the growth plate cartilage in the proximal tibias of three-week-old mice were immunostained with an anti-Cyp26b1 antibody (Red). The blue color is Hoechst stain, which indicates nuclei. Bars: 100 μm. (E, F) Effects of a vitamin A-deficient diet on the growth plate cartilage of *Cyp26b1*$^{\Delta chon}$ cKO mice. The mothers of *Cyp26b1*$^{\Delta chon}$ cKO pups were fed with a vitamin A-deficient diet or a control diet from eight weeks before gestation until the sacrifice of the *Cyp26b1*$^{\Delta chon}$ cKO pups three weeks after birth. The pups consumed either their mother's milk or shared an identical diet with their mother. (E) *Left*, BrdU was injected intraperitoneally into the mice two hours before sacrifice. Top, hematoxylin–eosin staining. Bottom, semiserial sections were immunostained with an anti-BrdU antibody. Regions corresponding to the boxed regions in the top are magnified and shown. Bars: 100 μm. *Right*, ratios (%) of the number of BrdU-positive cells to the number of total cells in the proliferative chondrocyte zone. $^{/}P < 0.01$ ($n = 5$). (F) Mean ± S.D. of the height of the proliferative chondrocyte zone (left) and the hypertrophic chondrocyte zone (right). $^{//}P < 0.05$ ($n = 5$).

detectable or is limited in the primordial cartilage during the embryonic stage [22], which is consistent with the normal embryonic development of *Cyp26b1*$^{\Delta chon}$ cKO mice in this study.

The partial recovery of growth plate abnormalities in *Cyp26b1*$^{\Delta chon}$ cKO mice by a vitamin A-deficient diet supports the notion that *Cyp26b1* deletion caused abnormalities through elevated RA activities in the growth plate. Accordingly, the decreased proliferation rates of proliferative chondrocytes in *Cyp26b1*$^{\Delta chon}$ cKO mice suggest that excess RA inhibits the proliferation of proliferative chondrocytes. Previous studies on the effects of RA have yielded conflicting data regarding its regulation of the differentiation of chondrocytes in the growth plate [23]. Ballock et al. reported that RA blocks the stimulatory effects of thyroid hormone on cultured rat chondrocyte hypertrophy [23], whereas others showed RA induces the hypertrophy of cultured chick chondrocytes [24,25]. Such in vitro culture experiments are affected by the pharmacological dosage of RA, variations in the species, culture conditions, composition of serum and the anatomical source of the growth plate cells used [23]. Our in vivo results are less susceptible to the above problems to better clarify the function of RA in chondrocyte proliferation/differentiation in the growth plate and in the bone growth.

Excess intake of vitamin A causes growth impairment and skeletal pain in juveniles [7–9]. Our study provides evidence that regulation of the RA distribution occurs within the growth plate cartilage and that this regulation plays critical roles in controlling the growth of long bones in juvenile mice. Our results also show that exogenous vitamin A can affect this regulation and distribution, since a vitamin A-deficient diet partially rescued the growth plate structure of *Cyp26b1*$^{\Delta chon}$ cKO mice. The characteristics of the closure of the growth plate seen in a child receiving excess RA [8] and guinea pigs receiving a RAR agonist [10] were similar

to those seen in *Cyp26b1*$^{\Delta chon}$ cKO mice in that the closure occurred in the central part of the growth plate, suggesting that a similar form of regulation occurs in humans and mice.

Acknowledgments

We thank Hiroshi Hamada and Satoru Mamiya for the *Cyp26b1* flox mice, Aki Takimoto, Chisa Shukunami and Yuji Hiraki for instructions about the cryostat sectioning, Janet Rossant for the RARE-LacZ mice, Peter Karagiannis for reading the manuscript, and Hiromi Kishi, Minoru Okada, Akihiro Yamashita and Miho Morioka for assistance and helpful discussions. This study was supported in part by the Japan Science Technology Agency (JST), CREST (to N.T.), Scientific Research Grant No. 23792042 (to Y. M.) and No. 24390354 (to N.T.) from MEXT.

References

[1] H. Fujii, T. Sato, S. Kaneko, O. Gotoh, Y. Fujii-Kuriyama, K. Osawa, S. Kato, H. Hamada, Metabolic inactivation of retinoic acid by a novel P450 differentially expressed in developing mouse embryos, EMBO J. 16 (1997) 4163–4173.

[2] W.J. Ray, G. Bain, M. Yao, D.I. Gottlieb, CYP26, a novel mammalian cytochrome P450, is induced by retinoic acid and defines a new family, J. Biol. Chem. 272 (1997) 18702–18708.

[3] J.A. White, Y.D. Guo, K. Baetz, B. Beckett-Jones, J. Bonasoro, K.E. Hsu, F.J. Dilworth, G. Jones, M. Petkovich, Identification of the retinoic acid-inducible all-trans-retinoic acid 4-hydroxylase, J. Biol. Chem. 271 (1996) 29922–29927.

[4] S. Shimozono, T. Iimura, T. Kitaguchi, S. Higashijima, A. Miyawaki, Visualization of an endogenous retinoic acid gradient across embryonic development, Nature 496 (2013) 363–366.

[5] Y. Sakai, C. Meno, H. Fujii, J. Nishino, H. Shiratori, Y. Saijoh, J. Rossant, H. Hamada, The retinoic acid-inactivating enzyme CYP26 is essential for establishing an uneven distribution of retinoic acid along the anterio-posterior axis within the mouse embryo, Genes Dev. 15 (2001) 213–225.

[6] K. Yashiro, X. Zhao, M. Uehara, K. Yamashita, M. Nishijima, J. Nishino, Y. Saijoh, Y. Sakai, H. Hamada, Regulation of retinoic acid distribution is required for proximodistal patterning and outgrowth of the developing mouse limb, Dev. Cell 6 (2004) 411–422.

[7] F. Luthi, Y. Eggel, N. Theumann, Premature epiphyseal closure in an adolescent treated by retinoids for acne: an unusual cause of anterior knee pain, Joint Bone Spine 79 (2012) 314–316.

[8] L.M. Milstone, J. McGuire, R.C. Ablow, Premature epiphyseal closure in a child receiving oral 13-cis-retinoic acid, J. Am. Acad. Dermatol. 7 (1982) 663–666.

[9] J. Prendiville, E.A. Bingham, D. Burrows, Premature epiphyseal closure – a complication of etretinate therapy in children, J. Am. Acad. Dermatol. 15 (1986) 1259–1262.

[10] A.M. Standeven, P.J. Davies, R.A. Chandraratna, D.R. Mader, A.T. Johnson, V.A. Thomazy, Retinoid-induced epiphyseal plate closure in guinea pigs, Fundam. Appl. Toxicol. 34 (1996) 91–98.

[11] J.A. Williams, N. Kondo, T. Okabe, N. Takeshita, D.M. Pilchak, E. Koyama, T. Ochiai, D. Jensen, M.-L. Chu, M.A. Kane, J.L. Napoli, M. Enomoto-Iwamoto, N. Ghyselinck, P. Chambon, M. Pacifici, M. Iwamoto, Retinoic acid receptors are required for skeletal growth, matrix homeostasis and growth plate function in postnatal mouse, Dev. Biol. 328 (2009) 315–327.

[12] J.A. Williams, M. Kane, T. Okabe, M. Enomoto-Iwamoto, J.L. Napoli, M. Pacifici, M. Iwamoto, Endogenous retinoids in mammalian growth plate cartilage: analysis and roles in matrix homeostasis and turnover, J. Biol. Chem. 285 (2010) 36674–36681.

[13] J. Rossant, R. Zirngibl, D. Cado, M. Shago, V. Giguere, Expression of a retinoic acid response element-hsplacZ transgene defines specific domains of transcriptional activity during mouse embryogenesis, Genes Dev. 5 (1991) 1333–1344.

[14] T. Iwai, J. Murai, H. Yoshikawa, N. Tsumaki, Smad7 inhibits chondrocyte differentiation at multiple steps during endochondral bone formation and down-regulates p38 MAPK pathways, J. Biol. Chem. 283 (2008) 27154–27164.

[15] D. Ikegami, H. Akiyama, A. Suzuki, T. Nakamura, T. Nakano, H. Yoshikawa, N. Tsumaki, Sox9 sustains chondrocyte survival and hypertrophy in part through Pik3ca-Akt pathways, Development 138 (2011) 1507–1519.

[16] J. Okano, U. Lichti, S. Mamiya, M. Aronova, G. Zhang, S.H. Yuspa, H. Hamada, Y. Sakai, M.I. Morasso, Increased retinoic acid levels through ablation of Cyp26b1 determine the processes of embryonic skin barrier formation and peridermal development, J. Cell Sci. 125 (2012) 1827–1836.

[17] T. Kawamoto, Use of a new adhesive film for the preparation of multi-purpose fresh-frozen sections from hard tissues, whole-animals, insects and plants, Arch. Histol. Cytol. 66 (2003) 123–143.

[18] P.W.J. Peters, Double staining of fetal skeletons for cartilage and bone, in: H.J.M.D. Neuberg, T.E. Kwasigroch (Eds.), Methods in Prenatal Toxicology, Georg Thieme Verlag, Stuttgart, Germany, 1977, pp. 153–154.

[19] A.K. Verma, A. Shoemaker, R. Simsiman, M. Denning, R.D. Zachman, Expression of retinoic acid nuclear receptors and tissue transglutaminase is altered in various tissues of rats fed a vitamin A-deficient diet, J. Nutr. 122 (1992) 2144–2152.

[20] H.J. Dranse, A.V. Sampaio, M. Petkovich, T.M. Underhill, Genetic deletion of Cyp26b1 negatively impacts limb skeletogenesis by inhibiting chondrogenesis, J. Cell Sci. 124 (2011) 2723–2734.

[21] G. MacLean, H. Li, D. Metzger, P. Chambon, M. Petkovich, Apoptotic extinction of germ cells in testes of Cyp26b1 knockout mice, Endocrinology 148 (2007) 4560–4567.

[22] H.P. von Schroeder, J.N. Heersche, Retinoic acid responsiveness of cells and tissues in developing fetal limbs evaluated in a RAREhsplacZ transgenic mouse model, J. Orthop. Res. 16 (1998) 355–364.

[23] R.T. Ballock, X. Zhou, L.M. Mink, D.H. Chen, B.C. Mita, Both retinoic acid and 1,25(OH)2 vitamin D3 inhibit thyroid hormone-induced terminal differentiation of growth plate chondrocytes, J. Orthop. Res. 19 (2001) 43–49.

[24] M. Iwamoto, I.M. Shapiro, K. Yagami, A.L. Boskey, P.S. Leboy, S.L. Adams, M. Pacifici, Retinoic acid induces rapid mineralization and expression of mineralization-related genes in chondrocytes, Exp. Cell Res. 207 (1993) 413–420.

[25] M. Pacifici, E.B. Golden, M. Iwamoto, S.L. Adams, Retinoic acid treatment induces type X collagen gene expression in cultured chick chondrocytes, Exp. Cell Res. 195 (1991) 38–46.